Highlighting the interdependence between volumetric contribution of fragility and cooperativity for polymeric segmental relaxation

Jules Trubert, Liubov Matkovska, Allisson Saiter-Fourcin, Laurent Delbreilh

Highlighting the interdependence between volumetric contribution of fragility and cooperativity for polymeric segmental relaxation

Jules Trubert, Liubov Matkovska, Allisson Saiter-Fourcin, Laurent Delbreilh*

Univ Rouen Normandie, INSA Rouen Normandie, CNRS, Normandie Univ, GPM UMR 6634, F-76000 Rouen, France

(* Corresponding author, electronic mail: jules.trubert@univ-rouen.fr)

ABSTRACT

The blurring around the link between the isobaric fragility and the characteristic size of cooperative rearranging region for glass forming liquids has been cleared up by considering volumetric and thermal contributions of the structural relaxation. The measurement of these contributions is carried for three amorphous thermoplastic polymers using broadband dielectric spectroscopy under pressure, providing an understanding on the link between isobaric fragilities, glass transition temperatures and microstructures. The cooperative rearranging region (CRR) volume is calculated as a function of pressure using the extended Donth's approach, and the values are compared with the activation volume at the glass transition under different isobaric conditions. By combining these different results, a link between the chemical structure and the influence of pressure/temperature on the molecular mobility can be established. Furthermore, this study shows also a strong correlation between the activation volume, leading to the volumetric contribution of the isobaric fragility, and the CRR volume. Finally, this work highlights the influence of inter- and intra-molecular interactions on thermal and volumetric contributions of the isobaric fragility as a function of pressure.

INTRODUCTION

Even if the glass transition is present in many systems (metallic glasses, polymeric glasses, oxide glasses), some questions about the physical origin of the glass transition remain unanswered [1–6]. Experimentally, it reflects the viscous slowing down [7–9], i.e. the relaxation time τ of glass-forming liquids increases drastically around the glass transition during cooling. When the temperature decreases, the evolution of the relaxation times deviates from an Arrhenius to a super-Arrhenius behavior. This deviation expresses the change in the energy barrier driving the structural relaxation process. It is conventional to associate the glass transition temperature of the glass formers with a relaxation time of 100 s [10].

In order to get a better overview of the mechanisms involved at the glass transition, Angell introduced the fragility index m_P allowing to determine the sensitivity of the relaxation time to a temperature variation at the glass transition temperature T_g for a constant pressure [11]:

$$m_P = \left(\frac{d\, log_{10}(\tau)}{d\left(\frac{T}{T_g}\right)} \right)_P \Bigg|_{T=T_g} . \quad (1)$$

Supercooled liquids can be classified between "strong" and "fragile" behaviors. Strong glass forming liquids (with a low fragility index, m_P close to 16), have almost an Arrhenius behavior, i.e. the activation energy allowing relaxation is practically constant whatever the temperature. At the opposite for fragile liquids such as polymers, this activation energy increases with cooling. This increase is experimentally observed by a huge increase of relaxation times directly linked with a non-Arrhenius behavior, and it can be described by the Vogel-Fulcher-Tamman law (VFT) [12–14]:

$$\tau(T) = \tau_\infty \exp \frac{DT_0}{T - T_0}. \quad (2)$$

In this expression, τ_∞ is a pre-exponential factor corresponding to the theoretical relaxation time at infinite temperature, D is the steepness parameter, and T_0 the Vogel temperature associated with an infinitely slow structural relaxation. This law defines the divergence of the relaxation time when T tends towards T_0, temperature similar to the Kauzmann temperature T_K [15–18].

The entropic model of Adam and Gibbs has been proposed in order to explain the viscous slowing down [19]. This theory introduced the concept of cooperative rearranging region (CRR) by the idea that the lower the temperature, the greater the number of structural units that must move cooperatively for allowing the system to relax. From the thermal fluctuations, Donth developed an approach to estimate the CRR size at the calorimetric glass transition [20,21]. Then, this approach has been extended upper the glass transition temperature in supercooled liquids [22]. Recently, the characteristic length of a CRR noted ξ has been measured on polymers from quasi-elastic neutron scattering, and coincides with the one determined by the thermal fluctuation approach [23] proposed by Donth.

Another theoretical concept called the dynamic heterogeneity approach has been proposed to interpret the increase of relaxation time based on the presence of spatiotemporal fluctuations [24–26]. This approach states that in a supercooled liquid, some structural unit groups relax over long distances, when others are completely frozen. These sub-ensembles are spatially correlated, leading to correlated movements of these structural units. They can be characterized in terms of length scale by probing the correlated movements with dynamic susceptibility [27–31], or more precisely the number of molecules dynamically correlated over a time corresponding to the average relaxation time.

Among the theories trying to explain the viscous slowing down, the mode coupling theory (MCT) [32,33] expresses the existence of a crossover temperature T_C, at which the relaxation processes separate into a slow one, the structural relaxation (α-relaxation), whose relaxation time diverges from T_C, and a fast one, the secondary relaxation. The random first-order theory (RFOT) takes up the MCT and the entropic model of Adam and Gibbs [34,35]. RFOT uses a mean-field approach based on the principle that a glass-forming liquid has a multitude of sub-ensembles in an amorphous configuration, which can rearrange by themselves if they possess a sufficient

amount of energy. The size of these sub-ensembles increases with decreasing temperature, associated with a decrease in configurational entropy.
Finally, another approach is the dynamic facilitation [36]. It is based on the free volume theory formulated firstly by Doolittle [37–39]. Dynamic facilitation stipulates that a structural unit that has relaxed promotes the relaxation of one of its neighbors, such as free volume abled to move but vanishing at low temperature due to geometrical constraints. This approach leads to the design of a class of statistical models which are the kinetically constrained models (KCM) [40–42].
Although, isobaric fragility m_P (see **Equation (1)**) conveys the molecular mobility at the glass transition, it is not clearly correlated with the glass transition concepts, such as cooperativity and free volume approaches. Some studies have shown there is no direct link between these concepts and m_P for several glass-forming liquids by the use of NMR [43,44], dielectric spectroscopy [30,45,46], Raman and Brillouin scattering [47], photon-correlation spectroscopy [48] and molecular dynamic simulations [49,50]. In the literature, a possible reason of the decorrelation between m_P and glass transition is associated with the hypothesis of two separated contributions of isobaric fragility: thermal and volumetric. Hong et al. established an expression of m_P by considering both contributions [51]:

$$m_P = m_V + \frac{\Delta V^{\#}}{\ln 10\, k_B}\frac{\alpha_T}{\kappa}. \tag{3}$$

In this equation given the isobaric fragility m_P, the first term is the thermal contribution (isochoric fragility m_V) and the second one is the volumetric contribution, also noted $(m_P - m_V)$. Isochoric fragility m_V corresponds to the temperature sensibility of the α-relaxation at the glass transition and constant volume. The second term associated with the volumetric contribution considers only the physical parameters of the volume variations: $\Delta V^{\#}$ the activation volume; k_B the Boltzmann's constant, α_T the thermal volume expansivity and κ the compressibility. These two contributions have been determined in different studies to explain some m_P variations as the function of the polymer chemical structure [46,52–54]. Indeed, the density changes during a cooling at atmospheric pressure P_{atm}. These contributions require studying the glass forming liquids in isobaric or isochoric conditions [55,56].

Since Debye has defined that the dielectric relaxation was due to the reorientational motions of the molecular dipoles [57], broadband dielectric spectroscopy (BDS) measurement is widely used to follow the relaxation time τ (see **Equation (2)**) with the complex dielectric response after application of an outer electric field over a very broad range of frequency (10^{-6} to 10^{12} Hz) [58]. The use of this technique under controlled atmosphere enables to apply a complementary pressure control to the classical thermal control [59–64]. By this way, the pressure can be modified at constant temperature, reducing the space available for structural unit movements, and thus hindering relaxation. Especially, it allows calculating activation volume, analogous to the activation energy [65–67] and isochoric fragility m_V [68,69], where activation volume is defined by:

$$\Delta V^{\#} = k_B T \left(\frac{\partial ln\, \tau}{\partial P}\right)_T. \tag{4}$$

The isochoric fragility m_V is obtained by compensating the thermal expansion with compressing the system in order to remain at constant volume.
Most of time, studies using the two contributions of isobaric fragility estimated them at atmospheric pressure: The thermal contribution is associated with intramolecular interactions, and the volumetric one is linked to intermolecular interactions, i.e. associated with the CRR size [70,31,45].

In this study, we propose to determine experimentally the thermal (m_V) and the volumetric ($\Delta V^{\#}\alpha_T / \ln 10\, k_B\kappa$) contributions of isobaric fragility m_P, and to link them to the CRR size. For this purpose, we study through high pressure BDS three amorphous thermoplastics with different relaxation behaviors, i.e. different atmospheric isobaric fragilities m_P, glass transition temperatures T_g and numbers of equivalent relaxation units in a CRR (N_α) at P_{atm}. The poly(ethylene terephthalate glycol) PETg shows a rigid backbone chain where the poly(vinyl acetate) PVAc has a flexible one. The poly(lactide acid) PLA is halfway between PETg and PVAc in terms of rigidity. This flexibility difference is reflected proportionally with their glass transition temperature difference, yet PLA has a very high isobaric fragility, close to the PETg one (see **Table 1**). As the PVAc has been particularly studied in high pressure BDS [56,71,72], it had allowed to assess our results, and to extend the method to PETg and PLA. Since these materials are polymers, the dielectric manifestation of their glass transition is observed from the segmental dynamics.
As far as we know, there is no research on the pressure and temperature effects on T_g variations and dynamic behaviors for PLA and PETg. Thus, thermal and volumetric contributions of m_P are expressed as a function of pressure, and the values are related to the chemical structure. Furthermore, the CRR volumes are calculated in different isobaric conditions using the extended Donth's approach, and the values are confronted to the activation volume at the glass transition temperature. By combining these different results, we can establish a link between the chemical structure of the three polymers and the influence of coupled pressure/temperature on their molecular mobility.

EXPERIMENTAL SECTION

Materials. The three thermoplastic amorphous polymers chosen are the poly(lactide acid) PLA, the poly(ethylene terephthalate glycol) PETg and the poly(vinyl acetate) PVAc. The chemical structure of each sample is presented in **Figure 1**. The PLA was purchased from Nature Works in the form of pellets. It is PLA 4042D composed with 95,7% of L-lactide and 4,3% of D-lactide. This isomer ratio allows to avoid fast polymer crystallization. The PVAc powder was acquired from Aldrich Chemical Company. The PLA and PVAc were dried during 24 hours at 60 °C and 50 °C, respectively. Then, the samples were thermo-molded at 200 °C for the PLA and at 120 °C for the PVAc. The PETg was provided by Eastman Chemical Company directly in film form. The PETg is a co-polymer composed of cyclohexanedimethanol, ethylene glycol and terephthalic acid with a molar ratio of approximately 1:2:3. The PETg samples were dried at 60 °C during 24h. Differential scanning calorimetry (DSC) measurements confirmed that all the samples were amorphous before the dielectric measurements. The molecular weights, the glass transition temperatures, the densities and the isobaric fragilities m_P of the samples at atmospheric pressure P_{atm} and ambient temperature are given in **Table 1**.

Table 1. Sample Name, Molecular Weight M_W, Glass Transition Temperature T_g taken at the middle point of the ΔC_P step obtained from classical DSC measurements, density at ambient temperature, isobaric fragility m_P and number of structural units in a CRR noted N_α at T_g under atmospheric pressure.

Sample Name	M_W $[g/mol]$	$T_{g,\mathrm{mid}}$ $[K]$	$Density$ $[g/cm^3]$	m_P	N_α
PETg [73,74]	26 000	351,2	1,27	141 - 165	77
PLA [54,74]	188 000	331,2	1,25	140 - 155	266
PVAc [45,70,74,75]	500 000	313,0	1,19	75 - 95	225-273

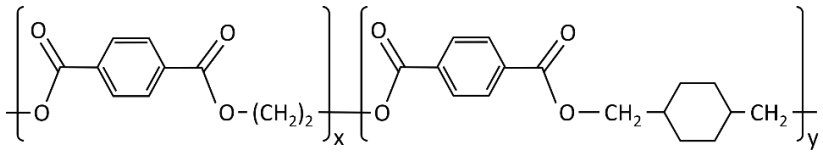

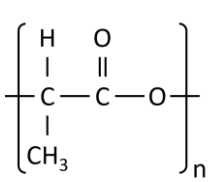

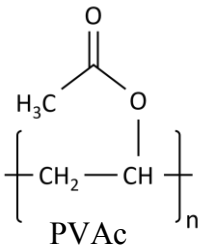

Figure 1. Structural unit of the polymers studied in this work. PETg have ratio of x = 2/3 and y = 1/3.

Dielectric relaxation spectroscopy under controlled pressure. The BDS measurements were carried out with a Novocontrol Alpha analyzer for frequency range between 10^{-1} Hz and 10^6 Hz. The samples were placed between two circular stainless-steel electrodes with a diameter of 15 mm. The electrodes were placed in a Teflon and polyisoprene assembly. It ensures the impermeability of the samples from oil (mixture of octane and silicone oil) in the high-pressure chamber. The pressure is applied to the oil in the chamber by piston, thus the pressure is hydrostatic. The device for applying pressure is the high-pressure pump U111 provided by UNIPRESS EQUIPMENT. The pressure is measured using a Nova Swiss tensiometer with a resolution of $\pm$ 0.1 MPa. The temperature is controlled by thermostatic bath and measured by means of a thermocouple with an accuracy of 0.1 K. To erase the thermal history and improve the material/electrode contact, the samples were annealed at a temperature 10 K above T_g during 10 min. Each sample was scanned in temperature, from 317 K up to 353 K for PVAc, from 337 K up to 353 K for PLA, and from 361 K up to 377 K for PETg. For each temperature step, dielectric measurements were performed for several pressures from 10 MPa up to the last pressure allowing a satisfactory view of the segmental relaxation. The last pressure varies as function of temperature, i.e. from 60 MPa up to 250 MPa for PVAc, from 30 MPa up to 130 MPa for PLA,

and from 30 MPa up to 95 MPa for PETg. Indeed, the crystallization of PLA and PETg samples prevent measurements with pressure higher than 130 MPa and 95 MPa respectively, whereas PVAc is able to be analyzed at higher pressure due to its constant fully amorphous nature. The Havriliak−Negami complex function (HN) [76] with a conductivity term was used in order to approximate the dielectric relaxation curves:

$$\varepsilon^*(\omega) = \varepsilon'(\omega) - i\varepsilon''(\omega) = -i\left(\frac{\sigma_0}{\varepsilon_0\omega}\right)^N + \sum_{k=1}^{2}\left[\frac{\Delta\varepsilon_k}{\left(1+\left(i\omega\tau_{HN,k}\right)^{\alpha_{HN,k}}\right)^{\beta_{HN,k}}}\right] + \varepsilon_\infty. \qquad (5)$$

In **Equation (5)**, ε^* is the complex permittivity, ω is the angular pulsation. ε^* can be expressed with ε' and ε'', the real and imaginary parts of complex permittivity, respectively. σ_0 accounts for the ohmic conduction related to the mobile charge carriers, N is a fitting parameter and ε_0 the dielectric permittivity of vacuum. $\Delta\varepsilon = \varepsilon_s - \varepsilon_\infty$ is the relaxation strength, where ε_s is the static permittivity (low frequency) and ε_∞ is the permittivity at high frequency. τ_{HN} is the relaxation time, α_{HN} and β_{HN} are the broadening and asymmetry factors, and k is the number of contributions needed to fit correctly the experimental data. These two contributions are associated with the segmental and the secondary relaxations.

RESULTS AND DISCUSSION

The relaxation time of segmental relaxations as the function of the pressure are plotted for PETg (**Figure 2a**), PLA (**Figure 2b**) and PVAc (**Figure 2c**) in isothermal conditions. Each point corresponds to the relaxation times τ_{HN} found by HN fit of the complex permittivity. The higher the temperature, the more visible the α-relaxation over a wide pressure range. According to the free volume concept, the molecular mobility is slowing down with an increase of the applied pressure at constant temperature. The free volume ratio should decrease and constrain the mobility. The pressure dependence of the relaxation time for the segmental relaxation can be described by the pressure VFT law [77–79] at constant temperature:

$$\tau(P) = \tau_0 \exp\frac{CP}{P_0 - P} \qquad (6)$$

where τ_0 corresponds to the relaxation time at atmospheric pressure (this parameter is set and determined from BDS measurements at P_{atm}), P_0 is the limit pressure where τ diverges, and C is a constant. The parameters of the pressure VFT law for isothermal measurements are given in the supplementary material (**Table S1**). For the three polymers, **Equation (6)** presents a nonlinear pressure dependence of the segmental relaxation time [80,81].

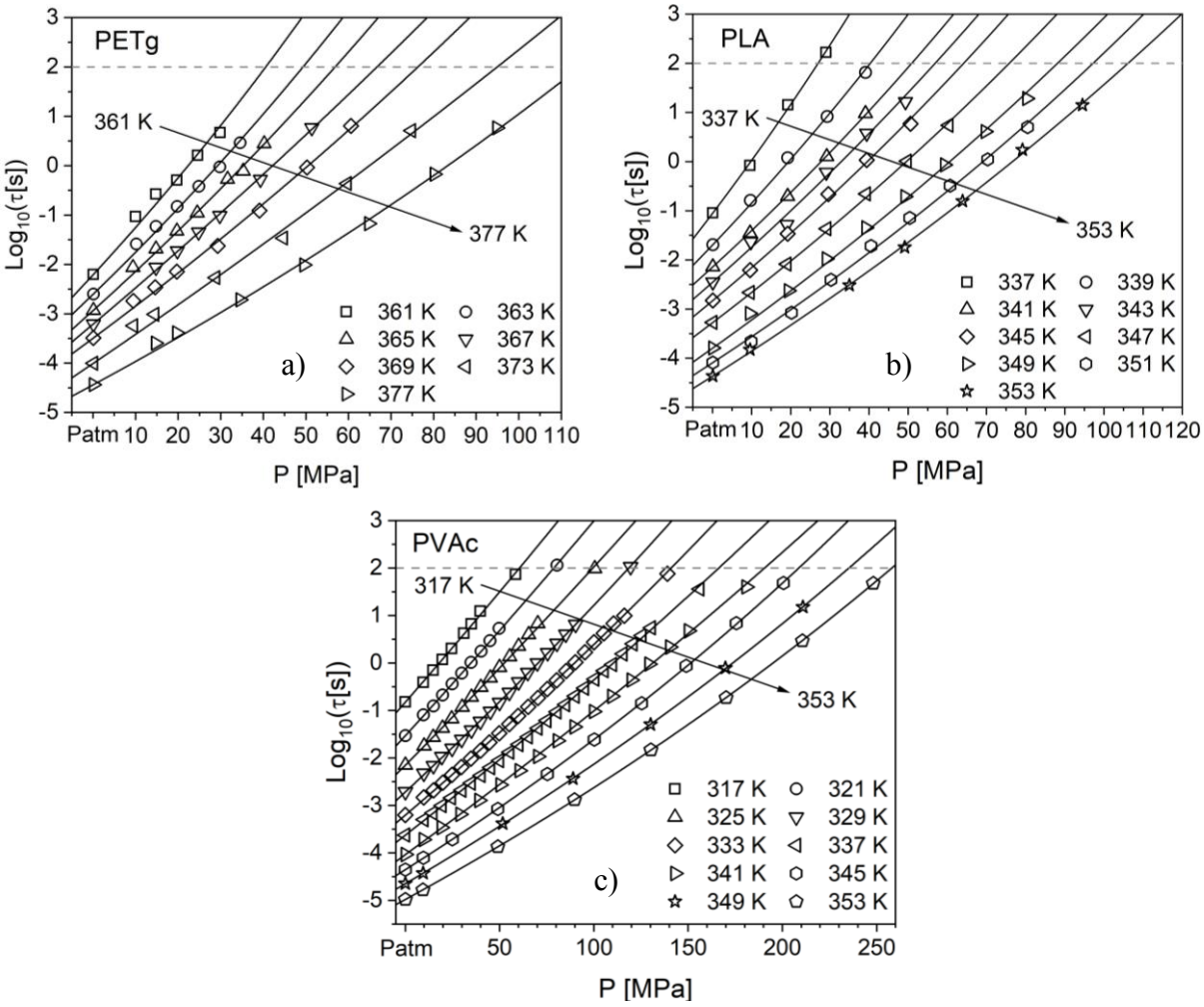

Figure 2. Pressure dependence of isothermal α-relaxation time for a) PETg, b) PLA and c) PVAc. The black lines are the pressure VFT fits for each isotherm. The dashed grey lines correspond to isochrone $\tau = 100\ s$, i.e. to the glass transition pressure P_g, analogous to the glass transition temperature T_g.

From **Equation (2)**, the temperature dependence of α-relaxation times can be deduced at constant pressure. **Figure 3** shows the isobaric evolution of the relaxation time extrapolated from the pressure VFT law (the law parameters are given in the supplementary material **Table S2**). The isobaric curves range from P_{atm} up to 70 MPa for PETg (**Figure 3a**), up to 100 MPa for PLA (**Figure 3b**) and up to 130 MPa for PVAc (**Figure 3c**). For the three polymers, the super-Arrhenius behavior of the segmental relaxation is well observed for each isobaric measurement.
The decrease of the temperature and the increase of the pressure have similar influences on molecular mobility. In both cases, the relaxation time is slowed down. When this slowing down process reaches the α-relaxation time of 100 s, the couple pression/temperature at this point is considered as the glass transition pressure P_g and the glass transition temperature T_g. By this way, a supercooled liquid can be turned into a glass by cooling down the material or by applying a hydrostatic pressure. The structure of the liquid remains "frozen", either because the system does not have enough configurational entropy to perform thermal fluctuations, or because it does not have enough space to perform spatial fluctuations.

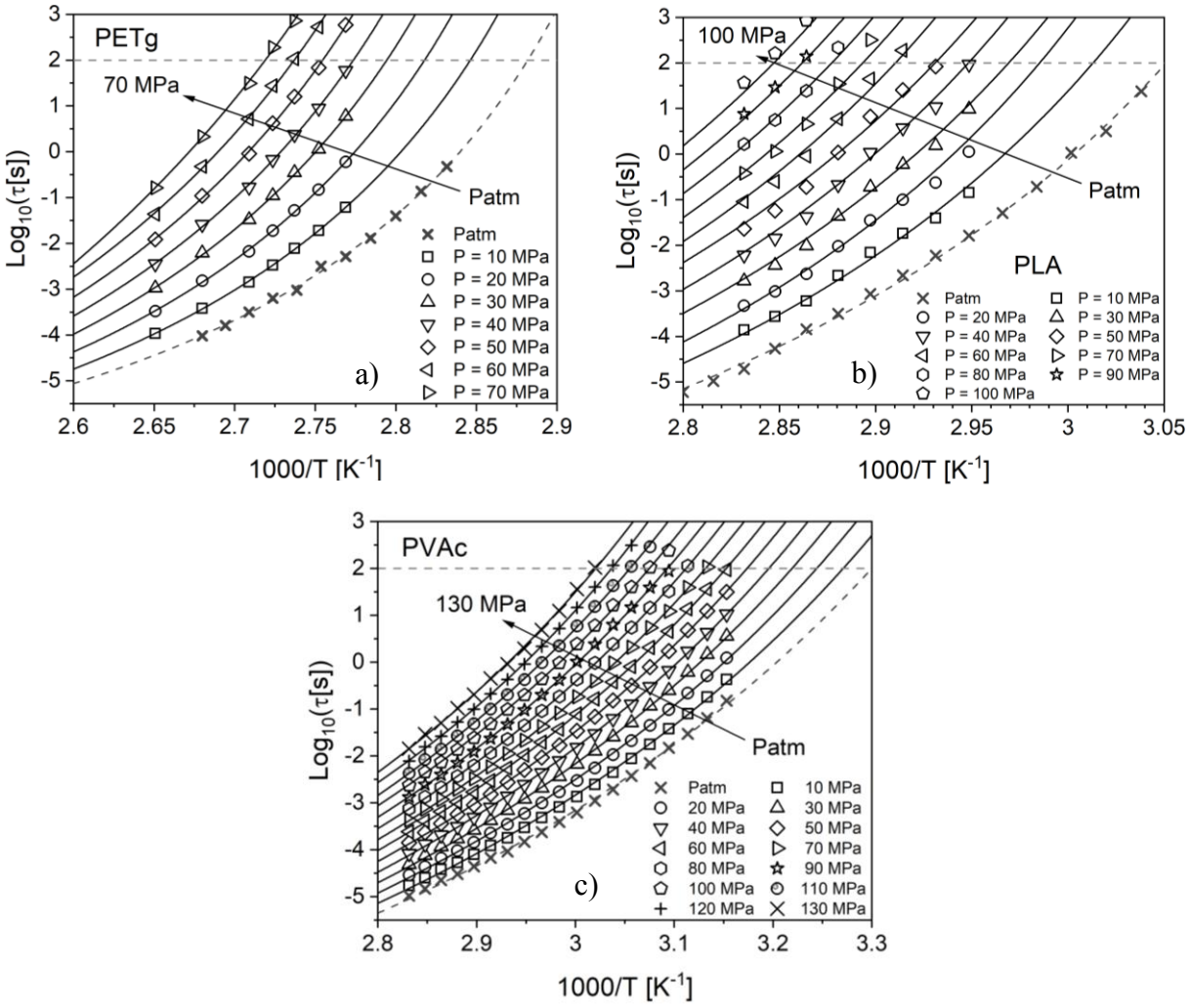

Figure 3. Temperature dependence of isobaric α-relaxation time τ for a) PETg, b) PLA and c) PVAc. The black lines are VFT fits of each isobar. The dashed black lines correspond to the VFT fit at P_{atm}. The dashed grey lines correspond to isochrone $\tau = 100\ s$, i.e. to the glass transition temperature T_g.

In **Figure 4**, the glass transition temperatures T_g of the three polymers determined through BDS analysis are plotted as a function of pressure. Overall, the glass transition temperature at $\tau = 100\ s$ increases with the pressure. T_g values are consistent with the literature [68], where $\mathrm{d}T_g/\mathrm{d}P$ is found between 0.1 and 0.4 $\mathrm{K.MPa^{-1}}$. However, the higher the pressure, the lower the increase of $T_g(P)$. This nonlinear behavior can be approximated by the Andersson's empirical model through the **Equation (7)** [82]:

$$T_g(P) = T_g^0 \left(1 + \frac{P}{\Pi}\right)^{\frac{1}{b}}, \tag{7}$$

where T_g^0 is the glass transition temperature at atmospheric pressure, Π and b are adjustable parameters. They are presented in the supplementary material (**Table S3**). This empirical

equation allows to depict the reduction of the T_g variation with the pressure increase. It has been shown that this model is a special case of the Avramov's model when $\tau = 100$ s [83,84]. In this latter model, Π and b are adjustable parameters with physical link expressed by $\Pi = C_P/(\alpha_T V_m b)$, where C_P is the heat capacity, α_T the thermal volume expansivity and V_m the molar volume. The parameter b from the Andersson's model is revealing of the T_g steepness variation as a function of pressure. It indicates that for PETg ($b = 11.2$), the value of $\mathrm{d}T_g/\mathrm{d}P$ decreases stronger than for PLA ($b = 7$), and PVAc ($b = 5.5$), when the pressure increases.

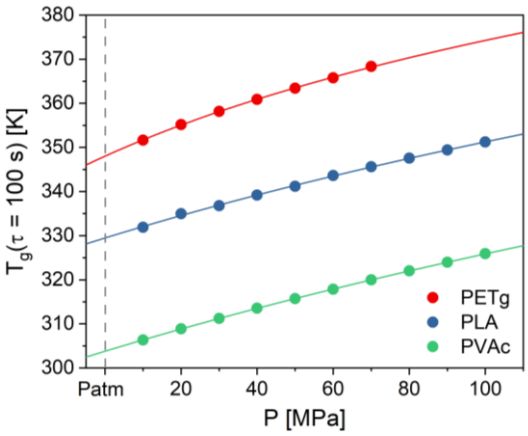

Figure 4. Glass transition temperature as a function of pressure for PETg in red, PLA in blue and PVAc in green. The lines correspond to the approximation of the experimental data with the Andersson's fit function.

Figure 5 shows the pressure influence on isobaric fragility m_P (see **Equation (1)**). There are clearly two behaviors: on one hand, PETg and PLA show high fragility at P_{atm}, then it decreases when the pressure increases. This behavior was expected according to previous studies [85,86]. On other hand, PVAc has relatively low isobaric fragility for a polymer, and the influence of pressure on m_P seems to be very low. Most of time, it has been showed that the isobaric fragilities of polymers decrease with pressure, however poly(ethyl acrylate) PEA, poly(butadiene) PBD and PVAc have $\mathrm{d}m_P/\mathrm{d}P = 0$ [87]. One can note these last three polymers have low m_P values at atmospheric pressure (PEA and PBD have isobaric fragilities of 83 and 67, respectively) and quite flexible backbone chain. Such behaviors seem not easy to relate directly to the structure of the repetitive unit (see **Figure 1**) because PLA shows a very high isobaric fragility, close to the one of PETg, despite an intermediate backbone rigidity between those of PETg and PVAc.

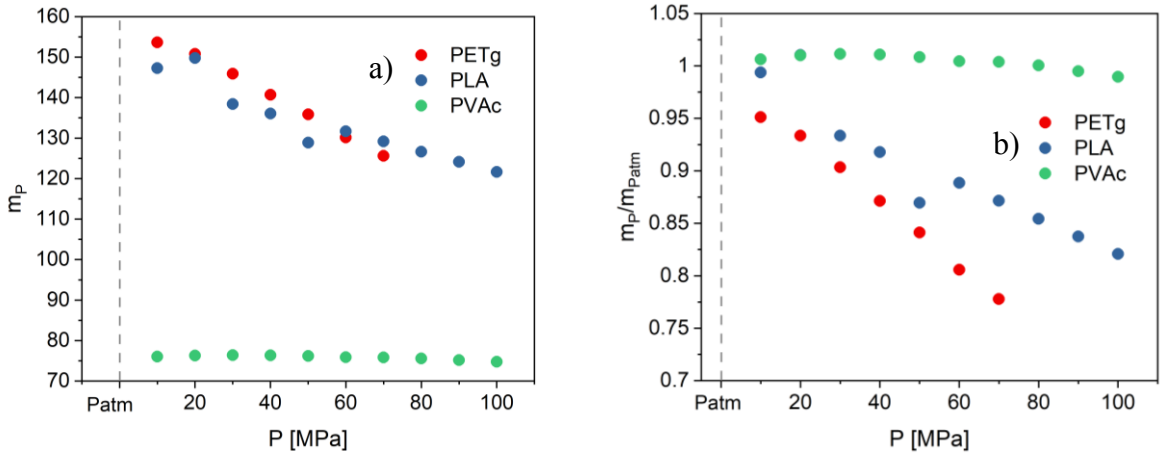

Figure 5. PETg in red, PLA in blue and PVAc in green. a) Isobaric fragility m_P as a function of pressure. b) Isobaric fragility normalized to the isobaric fragility at P_{atm} as a function of pressure.

Among the studies highlighting the uncorrelation between m_P and the glass transition concepts, Sokolov and co-workers [47,51] proposed an expression for m_P (see **Equation (3)**) as a function of the analogue isochoric fragility m_V, and a second contribution called $(m_P - m_V)$, involving the activation volume $\Delta V^{\#}$. $(m_P - m_V)$ is determined by considering the ratio α_T/κ at the glass transition temperature in a range from 1 up to 2 MPa/K for polymers [51]. The best match for the ratio is 1.5 MPa/K for PETg and PVAc, and 1.3 MPa/K for PLA. The activation volume $\Delta V^{\#}$ at T_g is determined from **Equation (8)**:

$$\Delta V^{\#} = m_P k_B \frac{\mathrm{d}T_g}{\mathrm{d}P} \ln 10. \tag{8}$$

In **Equation (8)** the glass transition temperature variation is obtained by using parameters of the Andersson's model such as:

$$\frac{\mathrm{d}T_g}{\mathrm{d}P} = \frac{T_g}{\Pi b \left(1 + \frac{P}{\Pi}\right)} \tag{9}$$

where Π and b are the same adjustable parameters than in **Equation (7)**. In **Equation (4)**, $\Delta V^{\#}$ must be calculated from the isothermal measurements (see **Figure 2**), whereas $\Delta V^{\#}$ calculated from **Equation (8)** is obtained through the isobaric measurements as shown in **Figure 3**. **Figure 6** guarantees both equations are consistent with each other. The variations of the activation volumes at T_g are similar to the ones reported by Roland and Casalini for PVAc, with activation volumes ranging from 0.217 up to 0.333 nm^3 for temperatures from 390 down to 340 K [88].

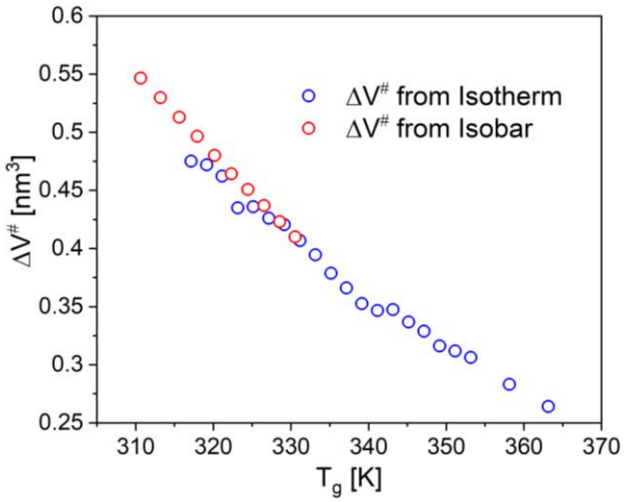

Figure 6. Activation volume $\Delta V^{\#}$ at the glass transition temperature T_g calculated form isothermal measurements and **Equation (4)** in empty blue circle, and from isobaric measurements and **Equation (8)** in empty red circles for PVAc.

The isobaric fragility and its two contributions are plotted as a function of pressure for PETg, PVAc and PLA (see **Figure 7**). Since $(m_P - m_V)$ decrease is steeper than the m_V increase, it induces a decrease of m_P for PETg and PLA, while these two contributions offset each other for PVAc, leading to the invariance of m_P with pressure. By rising the pressure, the two contributions of the isobaric fragility have two different behaviors. This difference between volumetric $(m_P - m_V)$ and thermal m_V contributions is expected for polymers [87] since the activation volume at the glass transition decreases when the pressure rises. The volumetric contribution $(m_P - m_V)$ does not favor the structural units to relax when pressure increases. On the other hand, in order to have a molecular mobility allowing relaxation fast enough to reach the glass transition, there must be a gain of energy to offset the deficit of activation volume at T_g. One can suggest that the thermal contribution of m_P increases with pressure to provide sufficient energy. Nevertheless, the isochoric fragility seems to converge to an asymptotic value at high pressure. This effect can be directly linked to the asymptotic behavior of the glass transition at high temperature [68,88,89].

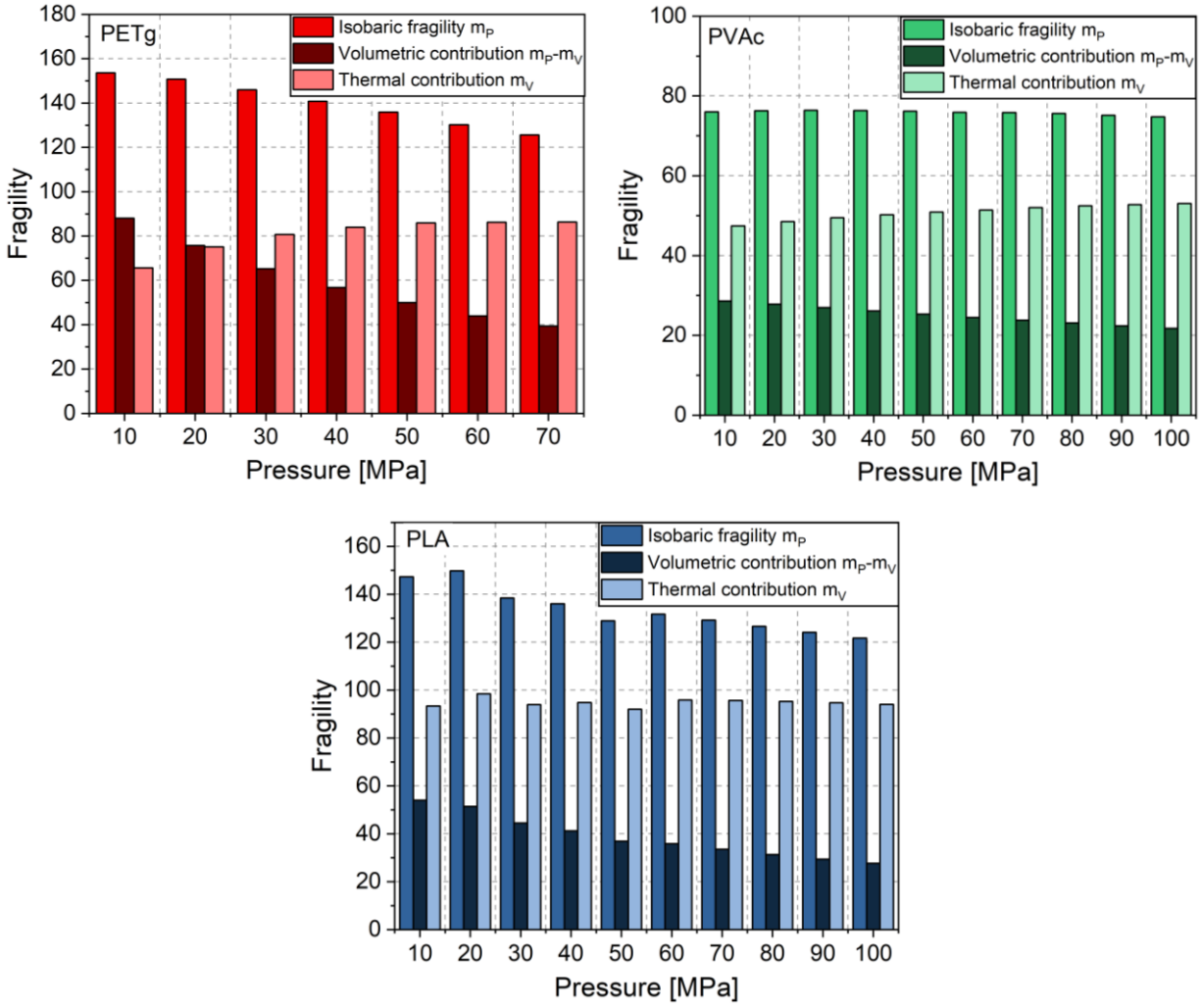

Figure 7. Isobaric fragility m_P and its volumetric $(m_P - m_V)$ and thermal m_V contributions as a function of pressure for PETg, PVAc and PLA.

The isochoric fragility m_V computed from the Angell's definition of the fragility is determined even if volume is unknown. In order to calculate m_V from **Equation (1)** adapted in isochoric conditions, the volume must be expressed as a function of pressure and temperature. For this purpose, the empirical Tait's equation [90] (see **Equation (10)**) allows approximating the PVT data, and defining the volume above T_g whatever the pressure and the temperature:

$$V(T,P) = V(T,\mathrm{P_{atm}})\left[1 - 0.0894 * \ln\left(1 + \frac{P}{B(T)}\right)\right]. \qquad (10)$$

The volume, in $mL.g^{-1}$, is expressed with the pressure, in bar. The volume at atmospheric pressure $V(T,P_{atm})$ and a pressure coefficient $B(T)$ are given by:

$$V(T,P_{atm}) = V_0 + V_1T + V_2T^2 \qquad \text{and} \qquad B(T) = b_0\exp(-b_1T). \qquad (11)$$

The PVT data for PLA and PVAc were extracted from the literature [91,92]. The Tait's equation for PETg was deduced from the density at ambient temperature and the second derivatives of free energy, i.e. the thermal volume expansivity α_T and the compressibility κ. The isothermal evolution of the segmental relaxation times can be transposed with the Tait's equation to the isochoric conditions.
From PVT data and the evolution of relaxation times with temperature and pressure, it is possible to proceed to a thermodynamic scaling [55,71,93–95]. It consists in expressing the relaxation time as a function of $T^{-1}V^{-\gamma}$, where γ is the scaling exponent corresponding to a material constant (refer to **Figure S1** for the thermodynamic scaling). γ is obtained from the expression: $\log(T_g) = A - \gamma \log(V_g)$ [86]. The scaling exponent can be used to express m_P as a function of m_V according to $m_P = m_V(1 + \alpha_T T_g \gamma)$ [94]. From the VFT fits (see **Figure 2**) and the PVT data given by Tait's equation, α-relaxation times were defined for constant volumes and approximated by VFT law. The isochoric fragilities are then determined from the Angell's definition (see **Equation (1)**). The agreement between isochoric fragilities obtained from **Equation (1)** and **Equation (3)** is detailed in **Figure S2.**

The higher the pressure, the lower the free and activation volumes. Thus, the distance between macromolecules is indubitably distorted. Thereby, the parameter $(m_P - m_V)$ is directly linked to the intermolecular interactions [46]. In literature, cooperativity has been related to intermolecular interactions [96–101]. Then, it seems interesting to follow cooperativity as a function of pressure, and to link it to the activation volume included in the expression of $(m_P - m_V)$ (see **Equation (3)**) in order to better understand the influence of interactions on the molecular mobility under pressure. Some studies have already suggested such connections [26,102], and defined a relation of $\Delta V^{\#} \approx (3 - 5\%)V_\alpha$ [46,51] for polymers. By combining Modulated Temperature Differential Scanning Calorimetry (MT-DSC) and BDS, Saiter et al. [22,103] proposed an extended Donth's approach [20] in order to determine the CRR volume V_α for any relaxational techniques:

$$V_\alpha = \frac{\left(\frac{1}{C_{P,glass}} - \frac{1}{C_{P,liquid}}\right) k_B T_\alpha^2}{\rho(\delta T)^2}, \tag{12}$$

where C_P is the specific heat capacity at constant pressure, k_B the Boltzmann's constant, the dynamic glass transition temperature, ρ the density, and δT the mean square temperature fluctuation associated with the glass transition. T_α and δT were determined by BDS analysis (method is detailed in the **Figure S3** of the Supplementary Material). The specific heat capacity is obtained from MT-DSC analysis, by extrapolating the liquid-like and glassy heat capacities at T_α. These values obtained from heat capacity measurements at atmospheric pressure can be used on a large range of pressure as observed in the literature [104].
Figure 8 displays the temperature dependence of the activation volume calculated from two methods. The first one consists in isobaric measurement using **Equation (8)**. For PVAc, the data were computed at $T_g = T(\tau = 10s)$, 10s corresponding to the equivalent relaxation time for MT-DSC measurements [45]. The second method uses $\Delta V^{\#} \approx (0.04 \pm 0.01) \times V_\alpha$ (see **Equation (12)** for V_α calculation) with a pressure range from the atmospheric pressure up to 50 MPa. A linear extrapolation of these data seems to reach the true activation volume at the conventional glass transition calculated from **Equation (8)**. At higher temperatures, the CRR volume converges to a

value close to the volume of a relaxing unit ($\Delta V^{\#} = 0.0048\ \mathrm{nm}^3$ and $V_\alpha = 0.12\ \mathrm{nm}^3$ for PVAc). The activation volume values at P_{atm} calculated from MT-DSC analyses match perfectly with the ones obtained by BDS measurements.

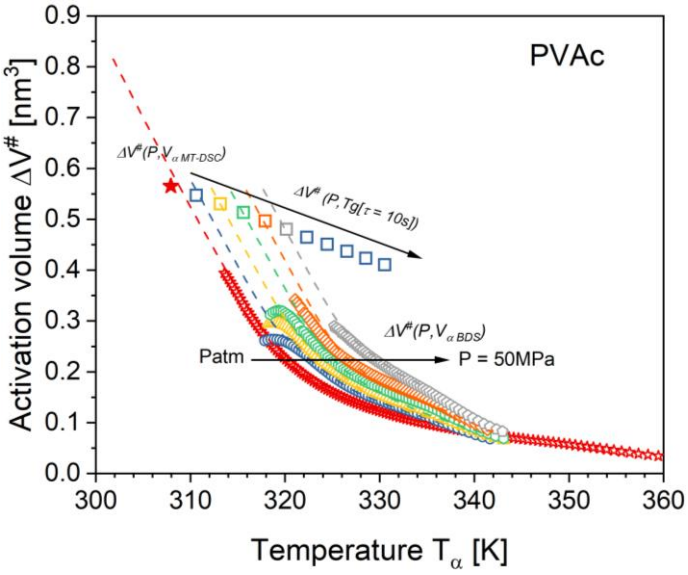

Figure 8. Activation volume $\Delta V^{\#}$ as a function of the temperature T_α for PVAc. The colored squares (☐) are the activation volumes for pressures from 10 MPa up to 100 MPa calculated from the **Equation (8)** and isobaric measurements at $\tau = 10s$. The red filled star (★) corresponds to $\Delta V^{\#} \approx 0{,}04 \times V_\alpha$ from MT-DSC measurements at P_{atm}. The empty symbols are associated with $\Delta V^{\#} \approx 0{,}04 \times V_\alpha$ determined from BDS analyses at P_{atm} (red empty stars), 10 MPa (blue circles), 20 MPa (yellow triangles), 30 MPa (green hexagons), 40 MPa (orange diamonds) and 50 MPa (grey pentagons). The dashed lines represent the extrapolation of $\Delta V^{\#}$ by this latter method at P_{atm}, transposed for the high pressure.

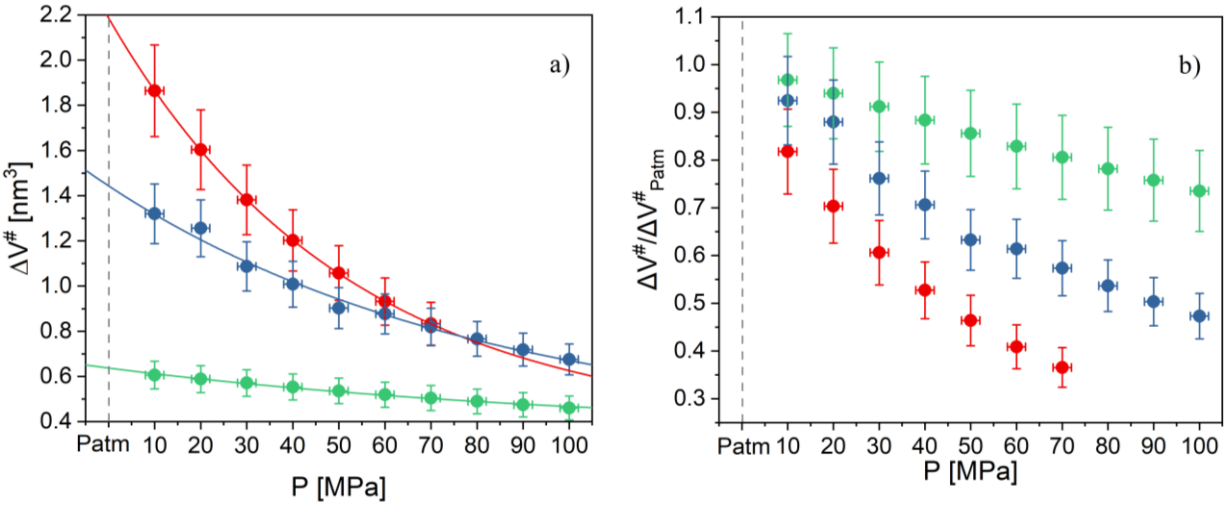

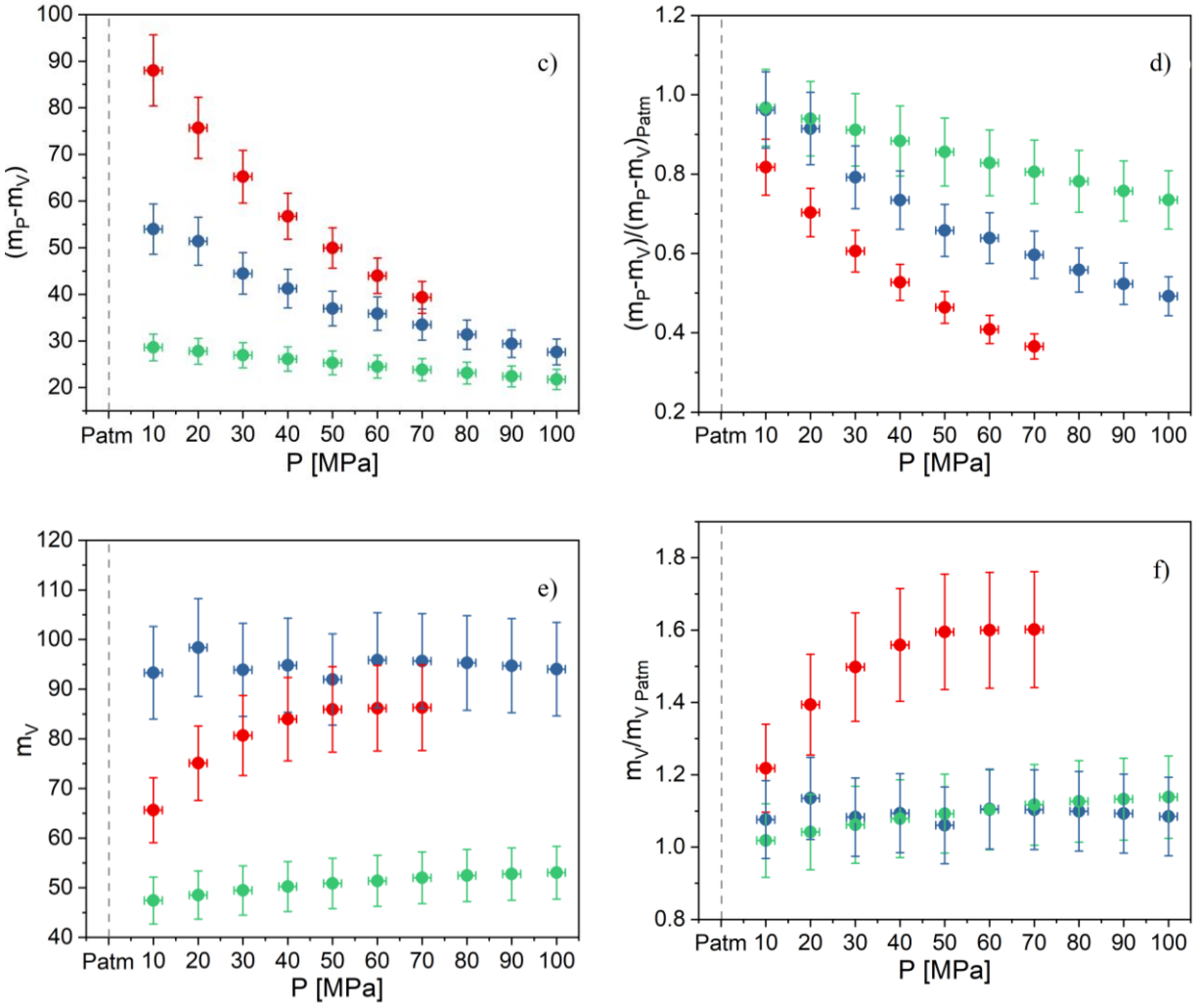

Figure 9. a) Activation volume $\Delta V^{\#}$ at $T_g(P)$ (the lines correspond to the one-phase exponential decay function), b) $\Delta V^{\#}$ normalized to its value at P_{atm}, c) volumetric contribution $(m_P - m_V)$, d) $(m_P - m_V)$ normalized to its value at P_{atm}, e) thermal contribution m_V and f) m_V normalized to its value at P_{atm} as the function of pressure for PETg in red, PLA in blue and PVAc in green.

Figure 9a displays the variations of the activation volume $\Delta V^{\#}$ as a function of pressure. Since this study has emphasized the direct correlation between activation volume and cooperativity size, PETg is the most cooperative at P_{atm} ($\Delta V^{\#} = 2.18$ nm^3), then PLA has intermediate cooperativity ($\Delta V^{\#} = 1.44$ nm^3), and PVAc has the lowest cooperativity ($\Delta V^{\#} = 0.64$ nm^3). These values have the same order of magnitude than those obtained by Rijal et al. [74]. Moreover, whatever the sample, the variations of $\Delta V^{\#}$ show an asymptotic behavior at high pressure, towards a value of 0.35 nm^3 corresponding to V_α = 8.75 nm^3 (more details about the fitting function are presented in the Supplementary Material). **Figure 9b** draws the activation volume at T_g ($\Delta V^{\#}$) normalized by the one at P_{atm} ($\Delta V^{\#}{}_{P_{\text{atm}}}$) as a function of pressure. PETg, which has the highest cooperativity, seems to be the most sensitive to the pressure. Conversely, PVAc is the one with the lowest variation as a function of pressure. **Figure 9c** shows the evolution of the

volumetric contribution $(m_P - m_V)$ with pressure, and **Figure 9d** shows this contribution normalized at $(m_P - m_V)_{P_{\mathrm{atm}}}$. Just like $(\Delta V^{\#})$, the more cooperative the polymer, the stronger the decrease of $(m_P - m_V)$. **Figures 9e** and **9f** show the thermal contribution m_V and this contribution normalized at $m_{V\,P_{\mathrm{atm}}}$ as a function of pressure, respectively. PLA shows a high isochoric fragility at P_{atm} and does not seem to vary so much with pressure. By contrast, m_V increases drastically before reaching a plateau for PETg, and m_V seems to increase slightly for PVAc, with values two times smaller than in the case of PLA. Thus, **Figure 9** indicates the higher the volumetric contribution $(m_P - m_V)$, the activation volume and so cooperativity, the stronger the decrease as a function of pressure. Since cooperativity is related to intermolecular interactions [96,97], the volumetric contribution is an indicator of intensity of these interactions. By increasing pressure, these intermolecular interactions become diminished, and then the cooperativity decreases [45,51,53,54]. However, Dudowicz et al.[105,106] and Kunal et al.[107] suggest the thermal contribution associated with the isochoric fragility m_V is related to the backbone flexibility, and therefore to intramolecular interactions. The question raised previously about an anomalous high m_P value at atmospheric pressure for PLA, seems to find part of the answer thanks to the thermal contribution calculation. Its isochoric fragility at P_{atm} is 86. By contrast, PETg and PVAc have values of 54 and 41, respectively. The value of thermal contribution m_V of isobaric fragility at P_{atm} does not seem to be related only to the backbone flexibility for PLA. This contribution may be rather related to the packing efficiency of polymers [107,108]. **Figure 7** shows that thermal contribution increases with the pressure until a certain pressure. It can be suggested that the convergence of this contribution towards a maximum could be explained by a minimum of activation volume, where a pressure increase is not sufficient anymore to change the volume. At this point, the thermal contribution allowing molecular mobility provides sufficient energy above the glass transition to proceed rearrangements, and should not increase further. Some studies showed an increase of isobaric fragility with pressure in non-polymeric glass forming liquids [109–112]. In metallic glasses, the structural network has metallic bonds that present a very different interatomic interactions nature [113]. Nevertheless, Roland et al. found that for normal liquids without strong H-bond, isobaric fragility should decreases with increasing pressure [55,68]. According to **Figure 8**, the activation volume seems to decrease faster at low temperature when the pressure increases. The red filled star corresponding to the activation volume at T_g and P_{atm} is equivalent to $N_\alpha = 167$. Since the activation volume at $T_g(P)$ decreases with pressure, cooperativity volume should reach in the worst scenario the value of a volume equivalent to $N_\alpha = 1$. In other words, at extremely high pressure, the volumetric contribution $(m_P - m_V)$ can decrease until reaching the same volumetric contribution than one relaxing unit. In this case, the isochoric fragility should be nearly equal to the isobaric fragility. At this point, m_P should reach a value around $60\sim90$ [114].

CONCLUSIONS

The molecular mobility of three thermoplastic polymers has been explored by separating the isobaric fragility m_P in its thermal m_V and volumetric $(m_P - m_V)$ contributions, using BDS under pressure. The activation volume $\Delta V^{\#}$ is the critical parameter allowing to calculate the volumetric contribution $(m_P - m_V)$. The connection between the CRR volume V_α as defined through the Donth's Model, and $\Delta V^{\#}$ calculated from the isobaric measurement is validated, and lengthened above the glass transition thanks to the extended Donth's approach. The cooperativity

seems to correlate better with the volumetric contribution of m_P, than with the isobaric fragility itself. Moreover, though the likeness of PLA and PETg at atmospheric pressure in terms of m_P, this study showed their isochoric fragilities m_V present variations drastically different with pressure. This work allows to correlate the fragility values at atmospheric pressure with the evolution of thermal and volumetric contributions. Thus, the high isobaric fragility values for PLA at atmospheric pressure can be related to its amount of thermal contribution associated with the backbone stiffness and the packing efficiency. Nonetheless, the volumetric contribution $(m_P - m_V)$, associated with the interchain interactions, decreases significantly when the pressure rises for PLA, PETg and PVAc. Both activation volume $\Delta V^{\#}$ and isobaric fragility m_P seem to converge respectively toward values of 0.35 nm^3 and $60{\sim}90$.

SUPPLEMENTARY MATERIAL

The Supplementary Material for this article is available online.

Thermodynamic scaling (**Figure S1**); Two methods for determining isochoric fragility m_V (**Figure S2**); Method for obtaining T_α and δT of the Donth's equation (**Figure S3**); Method for fitting activation volume $\Delta V^{\#}$ at T_g as a function of pressure.

Fit parameters of the pressure VFT law of **Figure 2** (**Table S1**); Fit parameters of the VFT law of **Figure 3** (**Table S2**); Fit parameters of the Andersson's empirical model of **Figure 4** (**Table S3**); Fit parameters of the one-phase exponential decay function of **Figure 4** (**Table S4**).

ACKNOWLEDGMENTS

The authors thank the University of Rouen and the Normandy Region for their financial support for Liubov Matkovska's position.

REFERENCES

[1] P.G. Debenedetti, and F.H. Stillinger, "Supercooled liquids and the glass transition," Nature **410**(6825), 259–267 (2001).
[2] E.-J. Donth, *The Glass Transition: Relaxation Dynamics in Liquids and Disordered Materials* (Springer Berlin Heidelberg, Berlin, Heidelberg, 2001).
[3] L. Berthier, and G. Biroli, "Theoretical perspective on the glass transition and amorphous materials," Rev. Mod. Phys. **83**(2), 587–645 (2011).
[4] J.C. Qiao, Q. Wang, J.M. Pelletier, H. Kato, R. Casalini, D. Crespo, E. Pineda, Y. Yao, and Y. Yang, "Structural heterogeneities and mechanical behavior of amorphous alloys," Progress in Materials Science **104**, 250–329 (2019).
[5] H. Lee, D. Son, S. Lee, K. Eun, M. Kim, and K. Paeng, "Utilization of Polymer-Tethered Probes for the Assessment of Segmental Polymer Dynamics near the Glass Transition," Macromolecules **55**(18), 8176–8185 (2022).
[6] P. Lunkenheimer, A. Loidl, B. Riechers, A. Zaccone, and K. Samwer, "Thermal expansion and the glass transition," Nat. Phys. **19**(5), 694–699 (2023).
[7] M.D. Ediger, C.A. Angell, and S.R. Nagel, "Supercooled Liquids and Glasses," J. Phys. Chem. **100**(31), 13200–13212 (1996).

[8] J.C. Dyre, "*Colloquium* : The glass transition and elastic models of glass-forming liquids," Rev. Mod. Phys. **78**(3), 953–972 (2006).
[9] T. Hecksher, A.I. Nielsen, N.B. Olsen, and J.C. Dyre, "Little evidence for dynamic divergences in ultraviscous molecular liquids," Nature Phys **4**(9), 737–741 (2008).
[10] L. Delbreilh, M. Negahban, M. Benzohra, C. Lacabanne, and J.M. Saiter, "Glass transition investigated by a combined protocol using thermostimulated depolarization currents and differential scanning calorimetry," J Therm Anal Calorim **96**(3), 865–871 (2009).
[11] C.A. Angell, "Spectroscopy simulation and scattering, and the medium range order problem in glass," Journal of Non-Crystalline Solids **73**(1–3), 1–17 (1985).
[12] hans Vogel, "Das Temperaturabhaengigkeitsgesetz der Viskositaet von Fluessigkeiten," Physikalische Zeitschrift **22**(645), (1921).
[13] G.S. Fulcher, "Analysis of recent measurements of the viscosity of glasses," J American Ceramic Society **8**(6), 339–355 (1925).
[14] G. Tammann, and W. Hesse, "Die Abhängigkeit der Viscosität von der Temperatur bie unterkühlten Flüssigkeiten," Z. Anorg. Allg. Chem. **156**(1), 245–257 (1926).
[15] Walter. Kauzmann, "The Nature of the Glassy State and the Behavior of Liquids at Low Temperatures.," Chem. Rev. **43**(2), 219–256 (1948).
[16] J.H. Gibbs, and E.A. DiMarzio, "Nature of the Glass Transition and the Glassy State," The Journal of Chemical Physics **28**(3), 373–383 (1958).
[17] R. Richert, and C.A. Angell, "Dynamics of glass-forming liquids. V. On the link between molecular dynamics and configurational entropy," The Journal of Chemical Physics **108**(21), 9016–9026 (1998).
[18] M. Goldstein, "Viscous Liquids and the Glass Transition: A Potential Energy Barrier Picture," The Journal of Chemical Physics **51**(9), 3728–3739 (1969).
[19] G. Adam, and J.H. Gibbs, "On the Temperature Dependence of Cooperative Relaxation Properties in Glass- Forming Liquids," The Journal of Chemical Physics **43**(1), 139–146 (1965).
[20] E. Donth, "The size of cooperatively rearranging regions at the glass transition," Journal of Non-Crystalline Solids **53**(3), 325–330 (1982).
[21] H. Huth, M. Beiner, S. Weyer, M. Merzlyakov, C. Schick, and E. Donth, "Glass transition cooperativity from heat capacity spectroscopy—temperature dependence and experimental uncertainties," Thermochimica Acta **377**(1–2), 113–124 (2001).
[22] A. Saiter, L. Delbreilh, H. Couderc, K. Arabeche, A. Schönhals, and J.-M. Saiter, "Temperature dependence of the characteristic length scale for glassy dynamics: Combination of dielectric and specific heat spectroscopy," Phys. Rev. E **81**(4), 041805 (2010).
[23] Y.Z. Chua, R. Zorn, J.W.P. Schmelzer, C. Schick, O. Holderer, and M. Zamponi, "Determination of Cooperativity Length in a Glass-Forming Polymer," ACS Phys. Chem Au **3**(2), 172–180 (2023).
[24] M.M. Hurley, and P. Harrowell, "Kinetic structure of a two-dimensional liquid," Phys. Rev. E **52**(2), 1694–1698 (1995).
[25] M.D. Ediger, "Spatially Heterogeneous Dynamics in Supercooled Liquids," Annu. Rev. Phys. Chem. **51**(1), 99–128 (2000).
[26] L. Berthier, "Time and length scales in supercooled liquids," Phys. Rev. E **69**(2), 020201 (2004).
[27] P. Mayer, H. Bissig, L. Berthier, L. Cipelletti, J.P. Garrahan, P. Sollich, and V. Trappe, "Heterogeneous Dynamics of Coarsening Systems," Phys. Rev. Lett. **93**(11), 115701 (2004).

[28] C. Dalle-Ferrier, S. Eibl, C. Pappas, and C. Alba-Simionesco, "Temperature dependence of three-point correlation functions of viscous liquids: the case of glycerol," J. Phys.: Condens. Matter **20**(49), 494240 (2008).
[29] S. Capaccioli, G. Ruocco, and F. Zamponi, "Dynamically Correlated Regions and Configurational Entropy in Supercooled Liquids," J. Phys. Chem. B **112**(34), 10652–10658 (2008).
[30] C. Crauste-Thibierge, C. Brun, F. Ladieu, D. L'Hôte, G. Biroli, and J.-P. Bouchaud, "Evidence of Growing Spatial Correlations at the Glass Transition from Nonlinear Response Experiments," Phys. Rev. Lett. **104**(16), 165703 (2010).
[31] Th. Bauer, P. Lunkenheimer, and A. Loidl, "Cooperativity and the Freezing of Molecular Motion at the Glass Transition," Phys. Rev. Lett. **111**(22), 225702 (2013).
[32] W. Gotze, and L. Sjogren, "Relaxation processes in supercooled liquids," Rep. Prog. Phys. **55**(3), 241–376 (1992).
[33] G. Biroli, and J.-P. Bouchaud, "Critical fluctuations and breakdown of the Stokes–Einstein relation in the mode-coupling theory of glasses," J. Phys.: Condens. Matter **19**(20), 205101 (2007).
[34] T.R. Kirkpatrick, and D. Thirumalai, "Dynamics of the Structural Glass Transition and the p - Spin—Interaction Spin-Glass Model," Phys. Rev. Lett. **58**(20), 2091–2094 (1987).
[35] V. Lubchenko, and P.G. Wolynes, "Theory of Structural Glasses and Supercooled Liquids," Annu. Rev. Phys. Chem. **58**(1), 235–266 (2007).
[36] G.H. Fredrickson, and H.C. Andersen, "Facilitated kinetic Ising models and the glass transition," The Journal of Chemical Physics **83**(11), 5822–5831 (1985).
[37] A.K. Doolittle, "Studies in Newtonian Flow. I. The Dependence of the Viscosity of Liquids on Temperature," Journal of Applied Physics **22**(8), 1031–1035 (1951).
[38] M.H. Cohen, and D. Turnbull, "Molecular Transport in Liquids and Glasses," The Journal of Chemical Physics **31**(5), 1164–1169 (1959).
[39] D. Turnbull, and M.H. Cohen, "Free- Volume Model of the Amorphous Phase: Glass Transition," The Journal of Chemical Physics **34**(1), 120–125 (1961).
[40] G.H. Fredrickson, and H.C. Andersen, "Kinetic Ising Model of the Glass Transition," Phys. Rev. Lett. **53**(13), 1244–1247 (1984).
[41] J. Jäckle, and S. Eisinger, "A hierarchically constrained kinetic Ising model," Z. Physik B - Condensed Matter **84**(1), 115–124 (1991).
[42] D. Kivelson, S.A. Kivelson, X. Zhao, Z. Nussinov, and G. Tarjus, "A thermodynamic theory of supercooled liquids," Physica A: Statistical Mechanics and Its Applications **219**(1–2), 27–38 (1995).
[43] U. Tracht, M. Wilhelm, A. Heuer, H. Feng, K. Schmidt-Rohr, and H.W. Spiess, "Length Scale of Dynamic Heterogeneities at the Glass Transition Determined by Multidimensional Nuclear Magnetic Resonance," Phys. Rev. Lett. **81**(13), 2727–2730 (1998).
[44] X.H. Qiu, and M.D. Ediger, "Length Scale of Dynamic Heterogeneity in Supercooled D - Sorbitol: Comparison to Model Predictions," J. Phys. Chem. B **107**(2), 459–464 (2003).
[45] J.A.S. Puente, B. Rijal, L. Delbreilh, K. Fatyeyeva, A. Saiter, and E. Dargent, "Segmental mobility and glass transition of poly(ethylene-vinyl acetate) copolymers: Is there a continuum in the dynamic glass transitions from PVAc to PE?," Polymer **76**, 213–219 (2015).

[46] S. Araujo, N. Delpouve, A. Dhotel, S. Domenek, A. Guinault, L. Delbreilh, and E. Dargent, "Reducing the Gap between the Activation Energy Measured in the Liquid and the Glassy States by Adding a Plasticizer to Polylactide," ACS Omega **3**(12), 17092–17099 (2018).
[47] L. Hong, P.D. Gujrati, V.N. Novikov, and A.P. Sokolov, "Molecular cooperativity in the dynamics of glass-forming systems: A new insight," J. Chem. Phys. **131**(19), 194511 (2009).
[48] C. Dalle-Ferrier, C. Thibierge, C. Alba-Simionesco, L. Berthier, G. Biroli, J.-P. Bouchaud, F. Ladieu, D. L'Hôte, and G. Tarjus, "Spatial correlations in the dynamics of glassforming liquids: Experimental determination of their temperature dependence," Phys. Rev. E **76**(4), 041510 (2007).
[49] L. Berthier, G. Biroli, J.-P. Bouchaud, L. Cipelletti, D.E. Masri, D. L'Hôte, F. Ladieu, and M. Pierno, "Direct Experimental Evidence of a Growing Length Scale Accompanying the Glass Transition," Science **310**(5755), 1797–1800 (2005).
[50] L. Berthier, G. Biroli, J.-P. Bouchaud, W. Kob, K. Miyazaki, and D.R. Reichman, "Spontaneous and induced dynamic correlations in glass formers. II. Model calculations and comparison to numerical simulations," The Journal of Chemical Physics **126**(18), 184504 (2007).
[51] L. Hong, V.N. Novikov, and A.P. Sokolov, "Is there a connection between fragility of glass forming systems and dynamic heterogeneity/cooperativity?," Journal of Non-Crystalline Solids **357**(2), 351–356 (2011).
[52] N. Delpouve, L. Delbreilh, G. Stoclet, A. Saiter, and E. Dargent, "Structural Dependence of the Molecular Mobility in the Amorphous Fractions of Polylactide," Macromolecules **47**(15), 5186–5197 (2014).
[53] S. Araujo, F. Batteux, W. Li, L. Butterfield, N. Delpouve, A. Esposito, L. Tan, J.-M. Saiter, and M. Negahban, "A Structural Interpretation of the Two Components Governing the Kinetic Fragility from the Example of Interpenetrated Polymer Networks," J. Polym. Sci. Part B: Polym. Phys. **56**(20), 1393–1403 (2018).
[54] S. Araujo, N. Delpouve, S. Domenek, A. Guinault, R. Golovchak, R. Szatanik, A. Ingram, C. Fauchard, L. Delbreilh, and E. Dargent, "Cooperativity Scaling and Free Volume in Plasticized Polylactide," Macromolecules **52**(16), 6107–6115 (2019).
[55] R. Casalini, and C.M. Roland, "Scaling of the supercooled dynamics and its relation to the pressure dependences of the dynamic crossover and the fragility of glass formers," Phys. Rev. B **71**(1), 014210 (2005).
[56] K. Niss, and C. Alba-Simionesco, "Effects of density and temperature on correlations between fragility and glassy properties," Phys. Rev. B **74**(2), 024205 (2006).
[57] P.J.W. Debye, *Polar Molecules* (Dover publications, 1929).
[58] F. Kremer, and A. Schönhals, editors , *Broadband Dielectric Spectroscopy* (Springer Berlin Heidelberg, Berlin, Heidelberg, 2003).
[59] G. Williams, "Complex dielectric constant of dipolar compounds as a function of temperature, pressure and frequency. Part 2.—The α–relaxation of polymethyl acrylate," Trans. Faraday Soc. **60**(0), 1556–1573 (1964).
[60] S. Saito, H. Sasabe, T. Nakajima, and K. Yada, "Dielectric relaxation and electrical conduction of polymers as a function of pressure and temperature," J. Polym. Sci. A-2 Polym. Phys. **6**(7), 1297–1315 (1968).
[61] H. Sasabe, and S. Saito, "Dielectric relaxations and electrical conductivities of poly(alkyl methacrylates) under high pressure," J. Polym. Sci. A-2 Polym. Phys. **6**(8), 1401–1418 (1968).

[62] M. Paluch, S. Hensel-Bielówka, and J. Zioło, "Effect of pressure on fragility and glass transition temperature in fragile glass-former," The Journal of Chemical Physics **110**(22), 10978–10981 (1999).
[63] A. Reiser, G. Kasper, and S. Hunklinger, "Effect of Pressure on the Secondary Relaxation in a Simple Glass Former," Phys. Rev. Lett. **92**(12), 125701 (2004).
[64] S. Capaccioli, M. Lucchesi, D. Prevosto, R. Casalini, and P. Rolla, "Effect of the isobaric and isothermal reductions in excess and configurational entropies on glass-forming dynamics," Philosophical Magazine **84**(13–16), 1513–1519 (2004).
[65] E.A. Guggenheim, "Thermodynamics of an activated complex," Trans. Faraday Soc. **33**, 607 (1937).
[66] M. Paluch, J. Gapinski, A. Patkowski, and E.W. Fischer, "Does fragility depend on pressure? A dynamic light scattering study of a fragile glass-former," The Journal of Chemical Physics **114**(18), 8048–8055 (2001).
[67] A. Drozd-Rzoska, "Activation volume in superpressed glass-formers," Sci Rep **9**(1), 13787 (2019).
[68] C.M. Roland, S. Hensel-Bielowka, M. Paluch, and R. Casalini, "Supercooled dynamics of glass-forming liquids and polymers under hydrostatic pressure," Rep. Prog. Phys. **68**(6), 1405–1478 (2005).
[69] K. Niss, C. Dalle-Ferrier, G. Tarjus, and C. Alba-Simionesco, "On the correlation between fragility and stretching in glass-forming liquids," J. Phys.: Condens. Matter **19**(7), 076102 (2007).
[70] E. Hempel, G. Hempel, A. Hensel, C. Schick, and E. Donth, "Characteristic Length of Dynamic Glass Transition near T_g for a Wide Assortment of Glass-Forming Substances," J. Phys. Chem. B **104**(11), 2460–2466 (2000).
[71] C. Alba-Simionesco, A. Cailliaux, A. Alegría, and G. Tarjus, "Scaling out the density dependence of the α relaxation in glass-forming polymers," Europhys. Lett. **68**(1), 58–64 (2004).
[72] R.P. White, and J.E.G. Lipson, "How Free Volume Does Influence the Dynamics of Glass Forming Liquids," ACS Macro Lett. **6**(5), 529–534 (2017).
[73] F. Hamonic, D. Prevosto, E. Dargent, and A. Saiter, "Contribution of chain alignment and crystallization in the evolution of cooperativity in drawn polymers," Polymer **55**(12), 2882–2889 (2014).
[74] B. Rijal, L. Delbreilh, and A. Saiter, "Dynamic Heterogeneity and Cooperative Length Scale at Dynamic Glass Transition in Glass Forming Liquids," Macromolecules **48**(22), 8219–8231 (2015).
[75] Q. Qin, and G.B. McKenna, "Correlation between dynamic fragility and glass transition temperature for different classes of glass forming liquids," Journal of Non-Crystalline Solids **352**(28–29), 2977–2985 (2006).
[76] S. Havriliak, and S. Negami, "A complex plane representation of dielectric and mechanical relaxation processes in some polymers," Polymer **8**, 161–210 (1967).
[77] M. Paluch, S.J. Rzoska, P. Habdas, and J. Ziolo, "Isothermal and high-pressure studies of dielectric relaxation in supercooled glycerol," J. Phys.: Condens. Matter **8**(50), 10885–10890 (1996).
[78] S. Corezzi, P.A. Rolla, M. Paluch, J. Zioło, and D. Fioretto, "Influence of temperature and pressure on dielectric relaxation in a supercooled epoxy resin," Phys. Rev. E **60**(4), 4444–4452 (1999).

[79] G.P. Johari, "Intrinsic mobility of molecular glasses," The Journal of Chemical Physics **58**(4), 1766–1770 (1973).
[80] M. Paluch, S.J. Rzoska, P. Habdas, and J. Ziolo, "On the isothermal pressure behaviour of the relaxation times for supercooled glass-forming liquids," J. Phys.: Condens. Matter **10**(19), 4131–4138 (1998).
[81] R. Casalini, M. Paluch, T. Psurek, and C.M. Roland, "Temperature and pressure dependences of the structural dynamics: an interpretation of Vogel–Fulcher behavior in terms of the Adam–Gibbs model," Journal of Molecular Liquids **111**(1–3), 53–60 (2004).
[82] S.P. Andersson, and O. Andersson, "Relaxation Studies of Poly(propylene glycol) under High Pressure," Macromolecules **31**(9), 2999–3006 (1998).
[83] I. Avramov, "Pressure dependence of viscosity of glassforming melts," Journal of Non-Crystalline Solids **262**(1–3), 258–263 (2000).
[84] G. Floudas, M. Paluch, A. Grzybowski, and K. Ngai, *Molecular Dynamics of Glass-Forming Systems* (Springer Berlin Heidelberg, Berlin, Heidelberg, 2011).
[85] C.M. Roland, and R. Casalini, "Effect of chemical structure on the isobaric and isochoric fragility in polychlorinated biphenyls," The Journal of Chemical Physics **122**(13), 134505 (2005).
[86] M. Paluch, K. Grzybowska, and A. Grzybowski, "Effect of high pressure on the relaxation dynamics of glass-forming liquids," Journal of Physics: Condensed Matter **19**(20), 205117 (2007).
[87] D. Huang, D.M. Colucci, and G.B. McKenna, "Dynamic fragility in polymers: A comparison in isobaric and isochoric conditions," The Journal of Chemical Physics **116**(9), 3925–3934 (2002).
[88] C.M. Roland, and R. Casalini, "Temperature and Volume Effects on Local Segmental Relaxation in Poly(vinyl acetate)," Macromolecules **36**(4), 1361–1367 (2003).
[89] M. Paluch, C.M. Roland, J. Gapinski, and A. Patkowski, "Pressure and temperature dependence of structural relaxation in diglycidylether of bisphenol A," The Journal of Chemical Physics **118**(7), 3177–3186 (2003).
[90] R.K. Jain, and R. Simha, "Theoretical equation of state: thermal expansivity, compressibility, and the Tait relation," Macromolecules **22**(1), 464–468 (1989).
[91] P. Zoller, and D.J. Walsh, *Standard Pressure-Volume-Temperature Data for Polymers* (Technomic Pub. Co, Lancaster, PA, 1995).
[92] J.E. McKinney, and R. Simha, "Configurational Thermodynamic Properties of Polymer Liquids and Glasses. I. Poly(vinyl acetate)," Macromolecules **7**(6), 894–901 (1974).
[93] R. Casalini, and C.M. Roland, "Scaling of the segmental relaxation times of polymers and its relation to the thermal expansivity," Colloid Polym Sci **283**(1), 107–110 (2004).
[94] R. Casalini, and C.M. Roland, "Thermodynamical scaling of the glass transition dynamics," Phys. Rev. E **69**(6), 062501 (2004).
[95] C.M. Roland, S. Bair, and R. Casalini, "Thermodynamic scaling of the viscosity of van der Waals, H-bonded, and ionic liquids," The Journal of Chemical Physics **125**(12), 124508 (2006).
[96] K.L. Ngai, and C.M. Roland, "Chemical structure and intermolecular cooperativity: dielectric relaxation results," Macromolecules **26**(25), 6824–6830 (1993).
[97] M. Nakanishi, and R. Nozaki, "Model of the cooperative rearranging region for polyhydric alcohols," Phys. Rev. E **84**(1), 011503 (2011).

[98] C.V. Grigoras, and A.G. Grigoras, "Nanoscale cooperativity on a series of statistical methacrylates copolymers with electron donor–acceptor pendant groups," J Therm Anal Calorim **103**(2), 661–668 (2011).
[99] K. Arabeche, L. Delbreilh, R. Adhikari, G.H. Michler, A. Hiltner, E. Baer, and J.-M. Saiter, "Study of the cooperativity at the glass transition temperature in PC/PMMA multilayered films: Influence of thickness reduction from macro- to nanoscale," Polymer **53**(6), 1355–1361 (2012).
[100] X. Monnier, N. Delpouve, N. Basson, A. Guinault, S. Domenek, A. Saiter, P.E. Mallon, and E. Dargent, "Molecular dynamics in electrospun amorphous plasticized polylactide fibers," Polymer **73**, 68–78 (2015).
[101] C. Liu, Z. Liu, X. Yin, and G. Wu, "Tuning the Dynamic Fragility of Acrylic Polymers by Small Molecules: The Interplay of Hydrogen Bonding Strength," Macromolecules **48**(12), 4196–4206 (2015).
[102] H. Zhang, and J.F. Douglas, "Glassy interfacial dynamics of Ni nanoparticles: part I Colored noise, dynamic heterogeneity and collective atomic motion," Soft Matter **9**(4), 1254–1265 (2013).
[103] A. Saiter, D. Prevosto, E. Passaglia, H. Couderc, L. Delbreilh, and J.M. Saiter, "Cooperativity length scale in nanocomposites: Interfacial and confinement effects," Phys. Rev. E **88**(4), 042605 (2013).
[104] O. Sandberg, and G. Bäckström, "Thermal conductivity and heat capacity of liquid and glassy poly(vinyl acetate) under pressure," J. Polym. Sci. Polym. Phys. Ed. **18**(10), 2123–2133 (1980).
[105] J. Dudowicz, K.F. Freed, and J.F. Douglas, "Fragility of Glass-Forming Polymer Liquids," J. Phys. Chem. B **109**(45), 21350–21356 (2005).
[106] J. Dudowicz, K.F. Freed, and J.F. Douglas, "Entropy theory of polymer glass formation revisited. I. General formulation," The Journal of Chemical Physics **124**(6), 064901 (2006).
[107] K. Kunal, C.G. Robertson, S. Pawlus, S.F. Hahn, and A.P. Sokolov, "Role of Chemical Structure in Fragility of Polymers: A Qualitative Picture," Macromolecules **41**(19), 7232–7238 (2008).
[108] J. Dudowicz, K.F. Freed, and J.F. Douglas, "The Glass Transition Temperature of Polymer Melts," J. Phys. Chem. B **109**(45), 21285–21292 (2005).
[109] S. Pawlus, M. Paluch, J. Ziolo, and C.M. Roland, "On the pressure dependence of the fragility of glycerol," J. Phys.: Condens. Matter **21**(33), 332101 (2009).
[110] Y.-C. Hu, P.-F. Guan, Q. Wang, Y. Yang, H.-Y. Bai, and W.-H. Wang, "Pressure effects on structure and dynamics of metallic glass-forming liquid," The Journal of Chemical Physics **146**(2), 024507 (2017).
[111] A.D. Phan, K. Koperwas, M. Paluch, and K. Wakabayashi, "Coupling between structural relaxation and diffusion in glass-forming liquids under pressure variation," Phys. Chem. Chem. Phys. **22**(42), 24365–24371 (2020).
[112] S. Assouli, H. Jabraoui, T. El hafi, O. Bajjou, A. Kotri, M. Mazroui, and Y. Lachtioui, "Exploring the impact of cooling rates and pressure on fragility and structural transformations in iron monatomic metallic glasses: Insights from molecular dynamics simulations," Journal of Non-Crystalline Solids **621**, 122623 (2023).
[113] T. Rouxel, H. Ji, T. Hammouda, and A. Moréac, "Poisson's Ratio and the Densification of Glass under High Pressure," Phys. Rev. Lett. **100**(22), 225501 (2008).

[114] Y. Ding, V.N. Novikov, A.P. Sokolov, A. Cailliaux, C. Dalle-Ferrier, C. Alba-Simionesco, and B. Frick, "Influence of Molecular Weight on Fast Dynamics and Fragility of Polymers," Macromolecules **37**(24), 9264–9272 (2004).